TEM Sample Preparation for Atomic-Scale Imaging and Microstructural Analysis Using High-Resolution (S)TEM with TESCAN AMBER X 2 Plasma FIB-SEM

F. Theska[1], A. I. Kamalasanan Pillai[1], J. Qu[1], M. Garbrecht[1], B. Saha[2], H. Wang[3], C. Sen[3], V. Bhatia[1]

[1] Sydney Microscopy & Microanalysis, The University of Sydney, Sydney NSW 2006, Australia
[2] Jawaharlal Nehru Centre for Advanced Scientific Research, India
[3] School of Photovoltaic & Renewable Energy Engineering, UNSW, Sydney NSW 2052, Australia

Introduction

Transmission electron microscopy (TEM) has been an integral part of materials research since its invention in the 1930's by Ernst Ruska and Max Knoll due to its unique ability to image materials at the atomic scale, revealing structural information at resolutions not attainable with other techniques (Williams and Carter, 2009). With the addition of complementary techniques such as Energy-Dispersive X-ray Spectroscopy (EDXS), electron diffraction (ED), or in-situ dynamic testing (e.g., changing temperature, biasing, or environmental) TEM has become an extremely powerful tool in materials research. However, TEM sample preparation plays a critical role in TEM imaging and analysis and can be a delicate and time-consuming process.

Over the years, many methods have been employed to prepare extremely thin and electron transparent samples for TEM. More recently, focused ion beam – scanning electron microscopes (FIB-SEMs) have greatly simplified the TEM sample preparation process using Ga ions for site-specific sputtering (Bassim et al., 2014). With the ability to locate regions of interest (ROIs) using the SEM and mill TEM lamellae using the FIB, this process has become simpler and increasingly automated (Cleeve et al., 2023). Ga FIBs offer high-resolution milling capabilities but can severely contaminate certain samples via Ga implantation and subsequent interdiffusion. While their milling accuracy is excellent, for other FIB applications the beam current range might be limiting.

In the last decade, the advent of the Xe Plasma FIB-SEM offers faster material removal rates that can be attributed to the higher atomic mass of Xe ions as well as a much wider range of beam currents. Another advantage of Xe Plasma FIBs is the non-reactivity of Xe, which minimizes ion beam -induced contamination considerably. Xenon Plasma FIB are also less likely to induce amorphization compared to Ga FIBs (Zhong et al., 2021). In general, Xe Plasma FIB offer a superior alternative to Ga FIBs in terms of sample integrity and high-throughput processing but cannot quite match the resolution.

This remained until the launch of TESCAN AMBER X 2 Plasma FIB-SEM (August 2024) featuring Mistral™ FIB column. The Mistral™ FIB column design features a significant improvement of resolution and beam profile across the ion energies, resulting in an focused ion beam spots that rivals the Ga FIBs, while retaining all the benefits of Xe plasma FIB.

In this application example, we demonstrate that thin films deposited on insulating substrates as well as porous metallization interfaces can be dealt with in a highly efficient manner using TESCAN AMBER X 2 at Sydney Microscopy & Microanalysis.

Materials & methods

The first sample was prepared from an $Al_{0.5}Sc_{0.5}N$ nitride thin film deposited on an insulating MgO substrate. The region of interest was the atomic-scale structure of the ~50 nm thin film and its monocrystalline substrate. This structure was synthesized via plasma-assisted molecular beam epitaxy. In preparation for the TEM lamella, a region of interest of ~10 µm length was protected first via electron beam Pt deposition at 2 kV, followed by ion beam Pt deposition at 10 kV.

Rough trenching was performed with an ion beam energy of 30 kV and current of 100 nA using Rectangular Polishing patterns in TESCAN DrawBeam™. Fine trenching used Rectangle Polishing at 30 kV and 20 nA.

A 'J-cut' was created using Lines to undercut the lamella and prepare it for in-situ lift-out using the OptiLift micro-manipulator. After successful lift-out, the lamella was attached to a Mo grid and thinned at 30 kV and successively reduced currents down to 100 pA.

Clean-up polishing was performed at 5 kV and 40 pA using a filled rectangle pattern under ±3.5° tilting, followed by 2 kV under ±5° tilting.

The second sample was prepared from an Ag metallization contact printed on a monocrystalline silicon solar cell. The region of interest was the interface between silicon substrate and Ag metallization exhibiting potential compositional variations or interdiffusion layers. To prepare a TEM lamella from a ~25 µm region of interest, electron and ion beam deposition were used.

Rough trenching was performed with an ion beam energy of 30 kV and 200 nA beam current using Rectangular Stairs patterns in TESCAN DrawBeam™. Fine trenching used Rectangle Polishing at 30 kV and 20 nA. Lines were used to undercut the lamella and prepare it for in-situ lift-out using the OptiLift micro-manipulator.

A 180° manipulator rotation allowed simple and fast preparation of an inverted lamella which was then attached to a Mo grid under -20° stage tilt. After successful lift-out, the lamella was thinned at 30 kV and successively reduced currents until 300 pA. Clean-up polishing was performed at 10 kV at 250 pA and 5 kV at 30 pA with a filled rectangle and ±5° stage over- and under-tilting.

TEM micrographs, STEM-HAADF micrographs, and STEM-EDXS maps were acquired with FEI Spectra 60-300 kV S/TEM and Themis-Z double-corrected 60-300 kV S/TEM instruments equipped with monochromator and SuperX-EDS detector systems for ultra-high-count rates operated at 300 kV.

Results & discussion

Figure 1a shows an exemplary TEM preparation of a $Al_{0.5}Sc_{0.5}N$ nitride thin film on an insulating MgO substrate. The Pt cap has been deposited densely to protect the region of interest below it. Preparation artefacts such as curtaining are mostly absent and this specimen is ready for in-situ lift-out. Figure 1b to c demonstrates the excellent TEM lamella quality after thinning and cleaning. The HR-TEM micrograph in Figure 1b reveals little to no bending or thickness variations across the field of view. The STEM HAADF micrograph in Figure 1c allows the identification of individual columns of atoms in $Al_{0.5}Sc_{0.5}N$ as well as MgO. The STEM HAADF micrograph in Figure 1d clearly reveals the atomic structure of the MgO substrate. Note that few to no steps were taken at this point to optimize the specimen preparation process.

Figure 2 demonstrates a more comprehensive visualization of the preparation of an inverted TEM lamella from a metallization contact on a silicon solar cell. Silicon substrate and silver contact are highlighted in Figure 2a. The region of interest is protected from ion beam damage with a Pt cap in Figure 2b. High current trenching and undercutting allow highly time efficient preparation of the region of interest for in-situ lift-out using the TESCAN OptiLift™ micromanipulator (see Figure 2c and d). At this stage, the porous structure of the silver metallization contact is revealed and expected to cause excessive preparation artefacts, such as curtaining. After the specimen is attached to the OptiLift micromanipulator, a 180° rotation allows to invert the TEM lamella in Figure 2e and f. Placing the porous silver metallization contact on the bottom of the lamella will minimize curtaining artefacts across the silicon substrate / silver contact interface. After attaching the inverted lamella to an Mo grid, thinning can proceed in Figure 2g. Once electron transparency is achieved, 10 kV and 5 kV clean-up allow to reduce amorphous damage

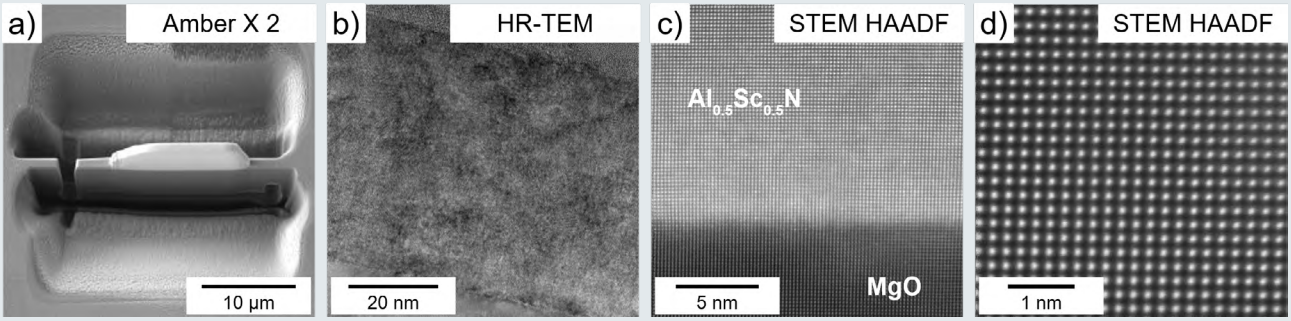

▲ **Figure 1:** TEM lamella preparation from $Al_{0.5}Sc_{0.5}N$ on a MgO substrate with the TESCAN AMBER X 2 Plasma FIB-SEM. a) Lamella ready for lift-out and thinning. b) HR-TEM micrograph of the cross-section. c) and d) STEM HAADF micrographs revealing exceptional specimen quality. Courtesy of Dr Bivas Saha (Jawaharlal Nehru Centre for Advanced Scientific Research, India), Ashalatha Indiradevi, and Dr Magnus Garbrecht (Sydney Microscopy & Microanalysis, The University of Sydney), under review (Manna et al., 2025).

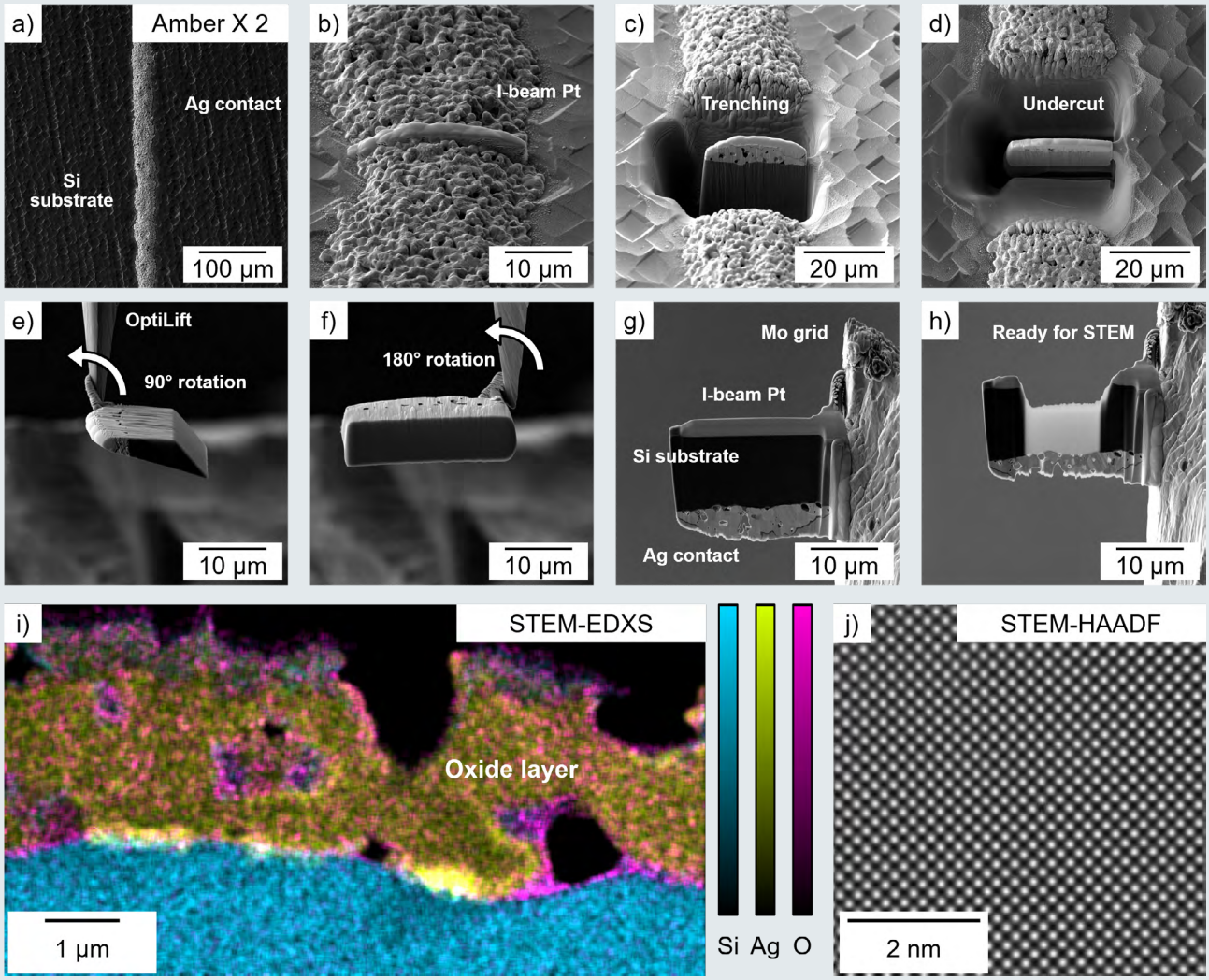

▲ **Figure 2:** Inverted TEM lamella preparation from an Ag metallization contact on a Si solar cell. a) to h) Specimen preparation with the TESCAN AMBER X 2 Xenon Plasma FIB equipped with TESCAN OptiLift™ micromanipulator. i) STEM-EDXS elemental mapping of an oxide layer below the Ag metallization and j) STEM HAADF micrograph revealing excellent specimen quality. Courtesy of Dr Chandany Sen, Haoran Wang (School of Photovoltaic & Renewable Energy Engineering, University of New South Wales (UNSW) Sydney), and Dr Jiangtao Qu (Sydney Microscopy & Microanalysis, The University of Sydney).

layers and Xe^+ ion implantation while thinning the specimen further until the desired thickness in Figure 2h. Finally, STEM-EDXS mapping reveals a thin oxide layer interacting with the interface between silicon substrate / silver metallization interface (Figure 2i). STEM-HAADF micrographs clearly show an absence of intrinsic defects in the atomic structure of the silicon substrate (Figure 2j).

Figure 3 provides a schematic representation of the inverted TEM lamella preparation presented in Figure 2. Initial protection of the region of interest is achieved by a Pt cap via e-beam deposition as highlighted by the active electron column in Figure 3a. This protective Pt cap is reinforced by a low-voltage deposition of Pt using the ion column in Figure 3b. This is followed directly by trenching at the same stage tilt. The individual pattern shape and type may depend on the individual sample that needs to be prepared; However, Rectangular or Trapezoid Stairs are recommended to reduce redeposition and provide a sufficient field of view to proceed with undercutting the lamella in Figure 3d. A small stage tilt allows users to observe when the undercutting is complete, and the lamella is ready for in-situ lift-out. As the OptiLift micromanipulator is positioned below the ion column it can be attached to the specimen under extremely shallow angles. The sample therefore must be flat and free of any protrusions. Concurrently, this approach allows users to simply rotate the TESCAN OptiLift™ micromanipulator by 180° to create an inverted TEM lamella (see Figure 3e). A tilt of -20° then allows to attach the lamella to a Mo or Cu grid in Figure 3f for subsequent thinning in Figure 3g. Low-voltage

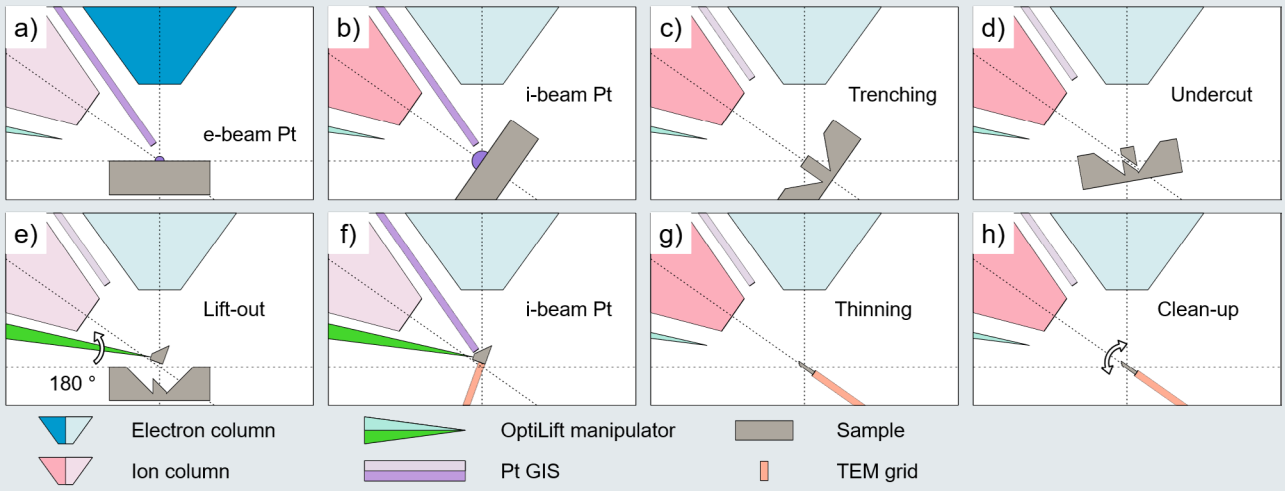

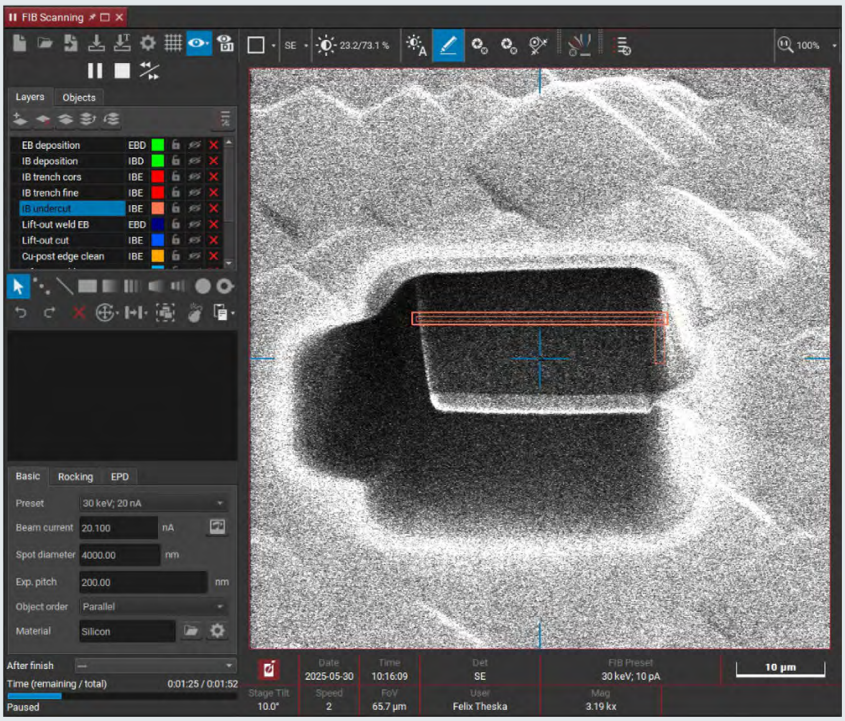

▲ **Figure 3:** Schematic of specimen preparation steps for an inverted TEM lamella. a) to g) Corresponding to Figure 2. h) TESCAN DrawBeam™ recipe template for streamlined preparation of similar specimens.

clean-ups may be performed using filled rectangle patterns with ±5° stage over- and under-tilting. This allows us to minimize amorphous damage layers and reduces ion implantation. Finally, TESCAN DrawBeam™ projects allow users to store the entire workflow as template ready to be applied to future sample preparation procedures. This can guide less experienced FIB users, but also saves valuable instrument time for expert users alike.

Finally, we have attempted a comparison of TEM lamella preparation procedures using a previous generation Ga FIB versus the latest generation TESCAN AMBER X 2 Plasma FIB-SEM. Time estimates have been averaged from TESCAN AMBER X over the preparation of eight TEM lamellae and have been compared to available ion beam current ranges of a previous generation FIB. A suitable agreement has been reached there with standard preparation routines. While the initial deposition of protective Pt caps consumes similar amounts of time for both instruments, considerable improvements were made during trenching with the Amber X 2. We attribute this to the remarkable ion beam profiles exhibiting low beam tails which allow the operation of x5 to x10 the usual ion beam current settings while maintaining comparable accuracy. This is followed by fine trenching, undercutting and in-situ lift-out. Here, small differences may be achieved, and exact time consumption strongly depends on the type of specimen to be prepared. After the lamella has been attached to a grid using ion beam Pt deposition, again,

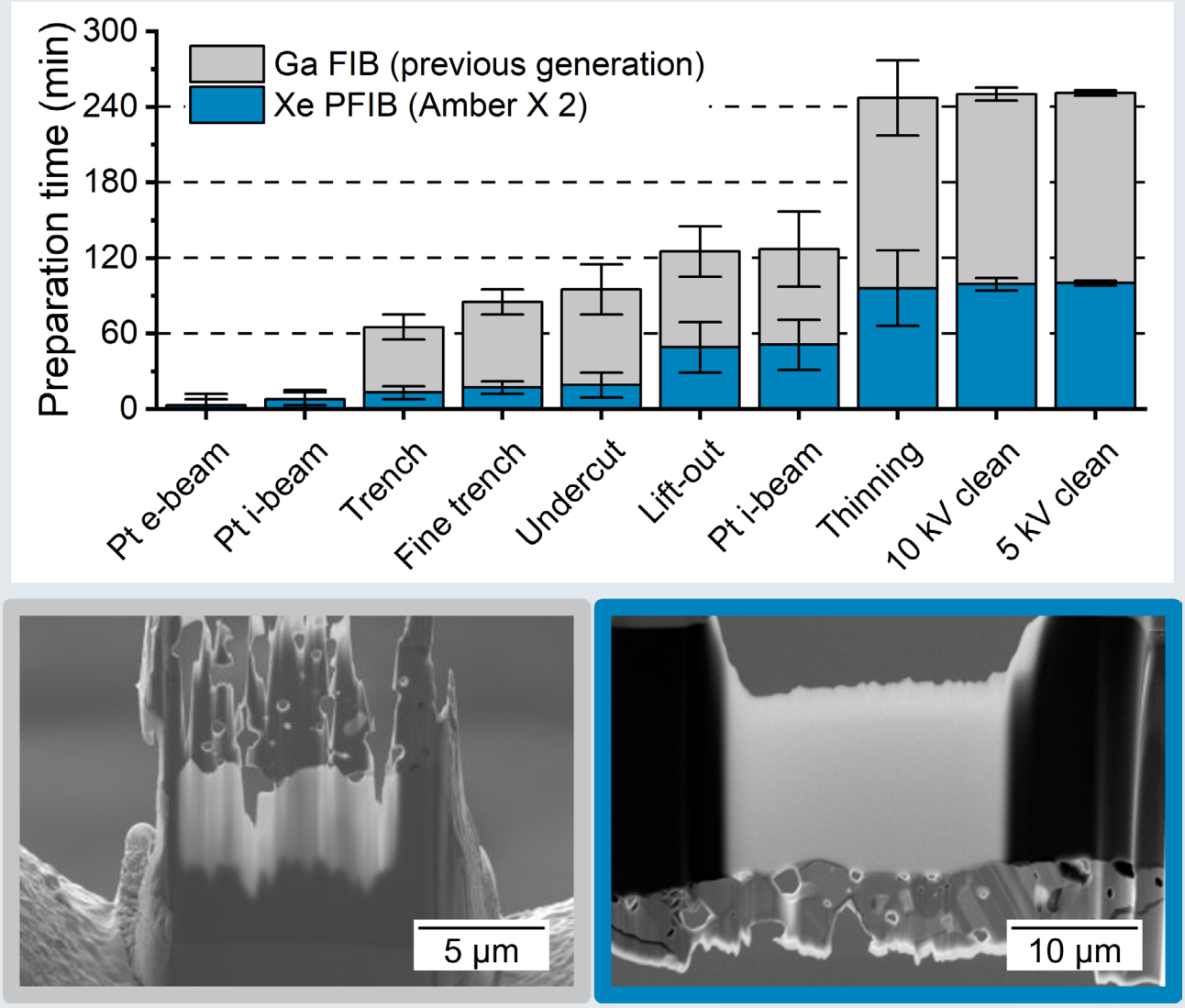

▲ **Figure 4:** Estimated cumulative time efforts for the TEM lamella preparation compared between a previous generation Ga^+ FIB and TESCAN AMBER X 2 latest generation Xe Plasma FIB. Preparing inverted TEM lamellae from porous metallization structures reduced curtaining artefacts considerably while maintaining an acceptable time effort.

the TESCAN AMBER X 2 allows significant improvements in preparation time by facilitating higher beam currents. Note that the current range is not unachievable by a previous generation Ga FIB per se, but rather TESCAN AMBER X 2 beam profiles allow a more aggressive approach at the benefit of preparation time. Finally, 10 kV and 5 kV clean-up procedures alike are comparable for both instruments again. However, it is noteworthy that a typical TEM lamella prepared using TESCAN AMBER X 2 takes between one and two hours, whereas a Ga FIB may require up to three hours to achieve similar dimensions-or necessitate preparing a significantly smaller specimen within the same time frame. Sydney Microscopy & Microanalysis typically offers researchers four-hour long sessions, meaning an experienced FIB operator may be able to double their specimen output or prepare significantly larger specimens and thus require fewer lift-outs and use their valuable TEM time more efficiently. Finally, the corresponding micrographs in Figure 4 demonstrate the value of access to simple and fast inverted TEM lamella preparation. FIB preparation artefacts, such as curtaining and lost material around the pores in the silver metallization contact are considerably minimized. If researchers are interested in the interface region between silicon substrate and silver contact, much more homogenous thickness profiles are achievable providing much more thorough investigation of these structures with the TEM.

Conclusions & outlook

TESCAN AMBER X 2 provides state-of-the-art Plasma FIB performance that rivals that of conventional FIB tools in several aspects and outperforms them in many. In a multi-user facility like Sydney Microscopy & Microanalysis, it has proven to be an invaluable asset complementing other FIB tools in the preparation of TEM lamellae in standard and inverted geometries.

Most outstanding is the precision and accuracy of the ion beam profiles enabling much more aggressive approaches resulting in significant time-savings while achieving uncompromised superior specimen quality. This translates into higher throughput and faster research outcomes.

Other key features of the system include TESCAN DrawBeam™ and FIB-SEM Expert PI. TESCAN DrawBeam™ projects guide less experienced researchers and save valuable time for expert users alike. Similarly, ExpertPI provides a simple interface allowing users to streamline their workflows by customizing the interface according to their needs and automate functions using a library of Python-based functions as well as enabling you to create your own scripts, thus simplifying complex operations.

3D FIB-SEM tomographic operations, specimen preparation for in-situ mechanical testing and atom probe sample preparation routines are being explored, and we are optimistic based on the success we have experienced thus far with the preparation of TEM lamellae.

References

Bassim, N., Scott, K., Giannuzzi, L.A., 2014. Recent advances in focused ion beam technology and applications. MRS Bull. 39, 317–325. https://doi.org/10.1557/mrs.2014.52

Cleeve, P., Dierickx, D., Naegele, L., Kannachel, R., Burne, L., Buckley, G., Gorelick, S., Whisstock, J.C., De Marco, A., 2023. OpenFIBSEM: A universal API for FIBSEM control. J. Struct. Biol. 215, 107967. https://doi.org/10.1016/j.jsb.2023.107967

Manna, S., Rudra, S., Das, P., Rao, D., Rawat, R., Dey, A., Pillai, A., Garbrecht, M., Saha, B., 2025. Electron-Doped Semiconducting Rocksalt AlxSc1-xN: A New Transparent Conducting Nitride (Under-Review 2025).

Williams, D.B., Carter, C.B., 2009. Transmission Electron Microscopy. Springer US, Boston, MA. https://doi.org/10.1007/978-0-387-76501-3

Zhong, X., Wade, C.A., Withers, P.J., Zhou, X., Cai, C., Haigh, S.J., Burke, M.G., 2021. Comparing Xe^+ pFIB and Ga^+ FIB for TEM sample preparation of Al alloys: Minimising FIB-induced artefacts. J. Microsc. 282, 101–112. https://doi.org/10.1111/jmi.12983

TESCAN GROUP, a.s.
Libušina tř. 21, 623 00 Brno - Kohoutovice / Czech Republic
(phone) +420 530 353 411 / (email) sales@tescan.com / marketing@tescan.com